

## Supporting information for “Patterned oscillating topographical changes in photoresponsive polymer coatings”

M. Hendrikx,<sup>a</sup> A. P. H. J. Schenning<sup>a</sup> and D. J. Broer<sup>a</sup>

<sup>a</sup> *Functional Organic Materials and Devices, Department of Chemical Engineering and Chemistry, Eindhoven University of Technology, 5612 AZAE, Eindhoven, The Netherlands and Institute for Complex Molecular Systems, Eindhoven University of Technology, P.O. Box 513, 5600 MB, Eindhoven, The Netherlands*

### **Polarized optical microscopy and birefringence of the photoaligned coatings**

The patterned LCN coatings are patterned prior to polymerization by utilizing a linear photopolymerizable polymer (LPP) as alignment layer. This layer is aligned prior to the filling and polymerization of the LC monomer mixture. After fixation of the alignment in the LCN the cell is opened and the coating is investigated by optical microscopy to determine the alignment direction of each domain and the optical properties of the adjacent domains (*i.e.* birefringence). The optical properties are determined with a Nikon Eclipse Ci equipped with a thermocontrolled stage (Linkam) and Berek Compensator. In Figure S1, the adjacent domains are shown with single polarizer and between both crossed polarizers. The alignment of the molecules inside the coating is determined with a single polarizer observation and the retardation,  $\Gamma = d\Delta n$ , of the coating is measured for both domains between crossed polarizers with a Berek compensator for a coating with a thickness of 6  $\mu\text{m}$ . The birefringence,  $\Delta n = n_e - n_o$ , found for both domains,  $0^\circ$  and  $90^\circ$ , is 0.198. This shows that both domains have the same optical properties, except for their alignment direction.

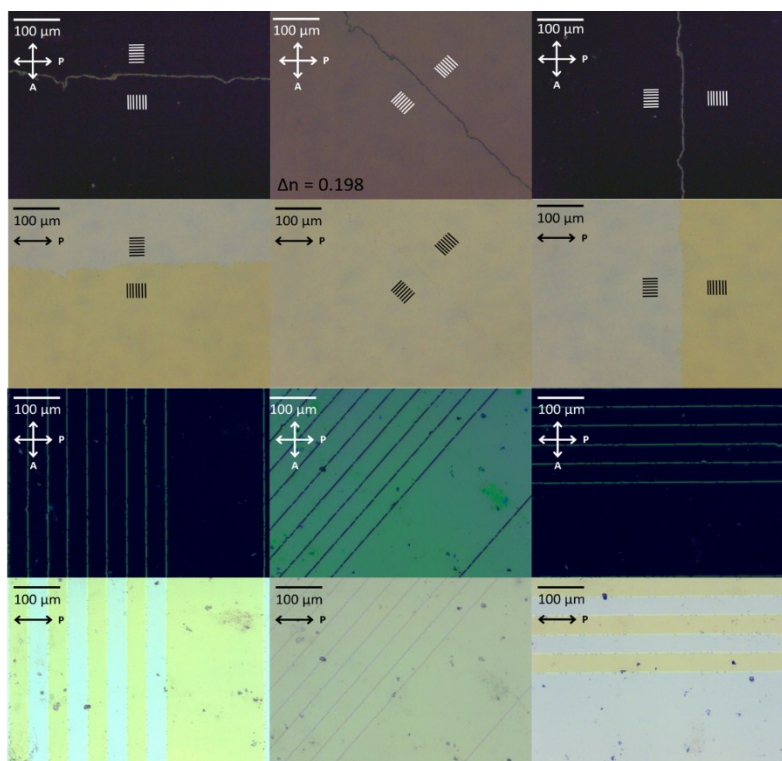


Figure S1: Polarized optical microscope images of 0/90 adjacent aligned liquid crystal coatings after opening of the LC cell. Arrows indicate the alignment of the polarizer (P) and analyzer (A). Solid lines (white and black) indicate the orientation of the alignment of the molecules inside the coating for the top 2 rows.

### Measurement of the dichroic ratio of the aligned samples

In order to understand the selective actuation, the ratio between the absorption of the azobenzene along the alignment of the liquid crystals and orthogonal to that must be known. This is expressed as the dichroic ratio (DR) of the light responsive coating. Here the DR is determined by UV/VIS, for this a uniaxial sample with a thickness of 2.1  $\mu\text{m}$  is prepared with the same materials as used for the other experiments. The parallel and perpendicular UV/VIS are shown in Figure S2. As reported in the main text, the dichroic ratio is 3.7 and 2.0 for 365 nm and 455 nm, respectively. The absorption observed for wavelengths below 325 nm result from the absorption of the polymeric backbone and glass.

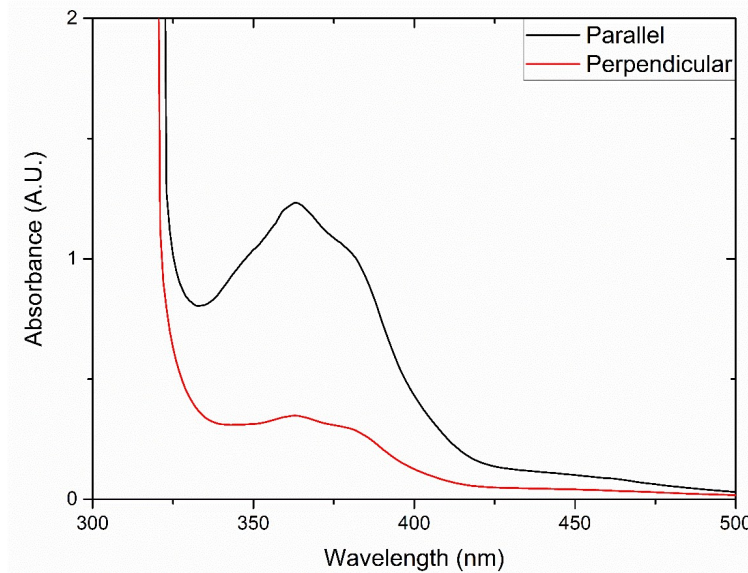


Figure S2: Parallel and perpendicular linear polarized absorption spectra of a uniaxial aligned 2  $\mu\text{m}$  coating.

### Digital Holographic Microscopy setup

Digital Holographic Microscopy (DHM) is a method to observe 3D images of surface in real-time. This 4D microscope allows us to determine height changes during illumination while monitoring the changes in dimensions of the coatings surface. The technique is based on the interference between a reflected beam that monitors the surface and a reference beam with the same overall path length. The reflected beam varies in path lengths due to the presence of topographies on the surface. As a result, the difference between the phase of the reflected and reference beam result in a hologram, captured by the camera. Through digital calculations, this hologram can be transformed into a 3D image of the surface. With the microscope working in reflection mode, there is no room to implement any necessary equipment underneath the objective due to the working distance (1.1 mm). Figure S3 shows the setup build for illumination before implementation in the DHM. The polarizer stage is detached from the thermocontrolled sample holder to remove any possible vibration originating from the rotating mechanics inside the polarizer stage.

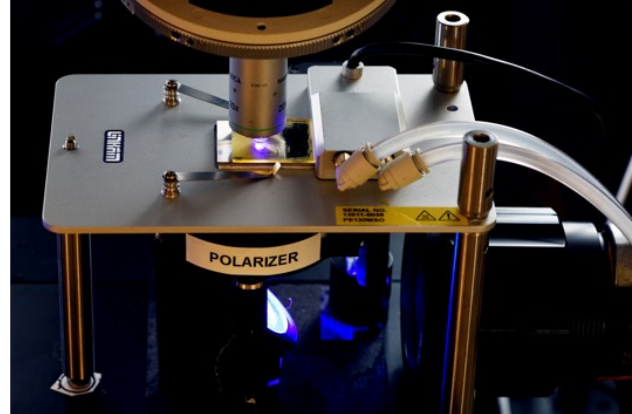
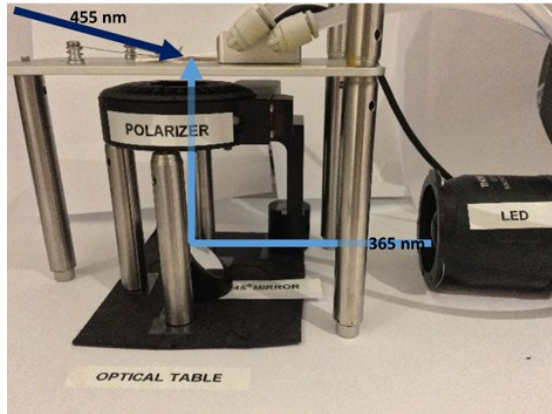


Figure S3: The setup build to illuminate the substrates while monitoring with DHM. The left picture shows the setup outside the DHM setup for clarity, on the right the setup is shown in combination with the DHM, for better illustration the 455 nm LED is turned off.

### **Lateral dimensions of the topographies**

For better understanding the effects of the topographic changes, profile extractions have been made of the experiments discussed in the main text. Here we show the lateral dimensions of the topographies achieved for 100  $\mu\text{m}$  and 20  $\mu\text{m}$  domain sized photoaligned coatings. As can be seen in Figure S4, one can clearly observe the final state (*i.e.* the last maximum in the oscillations) of the topographies, on the topological defect line between two adjacent 100  $\mu\text{m}$  domains, shows lateral dimensions of approx. 20  $\mu\text{m}$ . For the final state achieved for 20  $\mu\text{m}$  domains, one can clearly see that there is an asymmetric shape present with topographies over a full domain (*i.e.* 90° aligned).

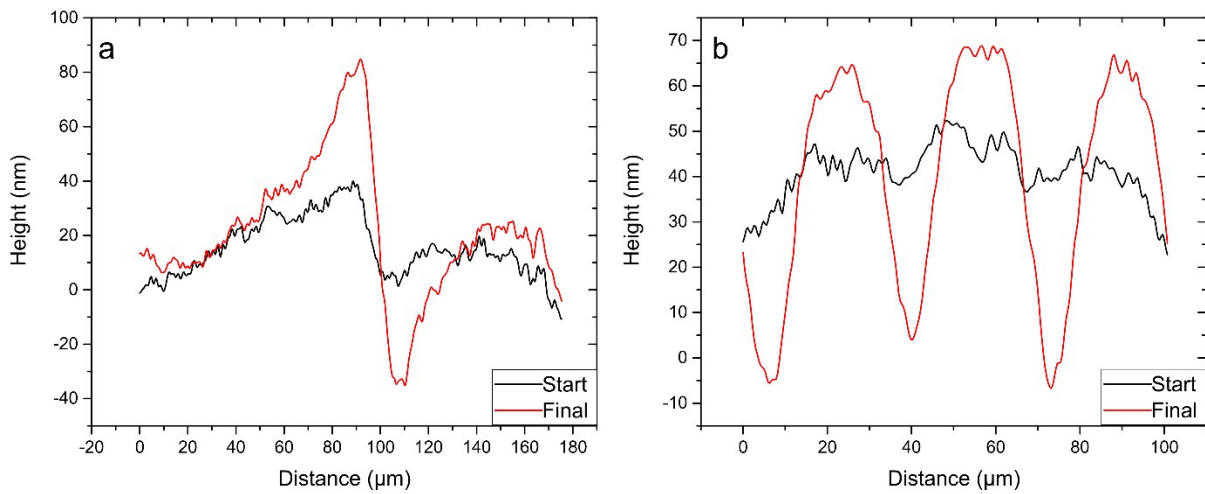


Figure S4: Profile of the topological defect lines at before illumination (start) and at the last maximum of the oscillations (finale) for (a) 100 μm and (b) 20 μm domains.

### Influence of the polarizer stage and polarization state of UV light

In order to understand the effect of the polarizer and illumination, multiple experiments have been performed in sequence to distinguish the individual effects. For these experiments a photoaligned coating with 20 μm domains has been used. Firstly none of the components have been addressed, the polarizer was removed from the stage and the stage was maintained stationary. Furthermore, no light was addressed. Figure S5 shows the successive results of turning individual components on and off. From  $t = 0$  s until  $t_1$  ( $= 591$  s), the setup and sample were held stationary. At  $t_1$  the polarizer was turned on and left to rotate at a speed of  $2.5^\circ \text{ s}^{-1}$  until  $t_2$  ( $= 1364$  s). The rotating stage was turned off from  $t_2$  until  $t_3$ . At this time, both the rotating stage without polarizer and the LEDs were turned on. As can be seen clearly, there is no change in height before  $t_3$ . After turning the LEDs on, the coating starts to deform. Here zone 1 decreases and zone 2 increases in height. Closer inspection leads to conclude zone 1 and zone 2 are oriented  $0^\circ$  and  $90^\circ$  to the topological defect line, respectively. This general trend is also seen in the

polarized UV light experiments. This proves that the oscillations originate from only the rotating linear polarized UV light exposure.

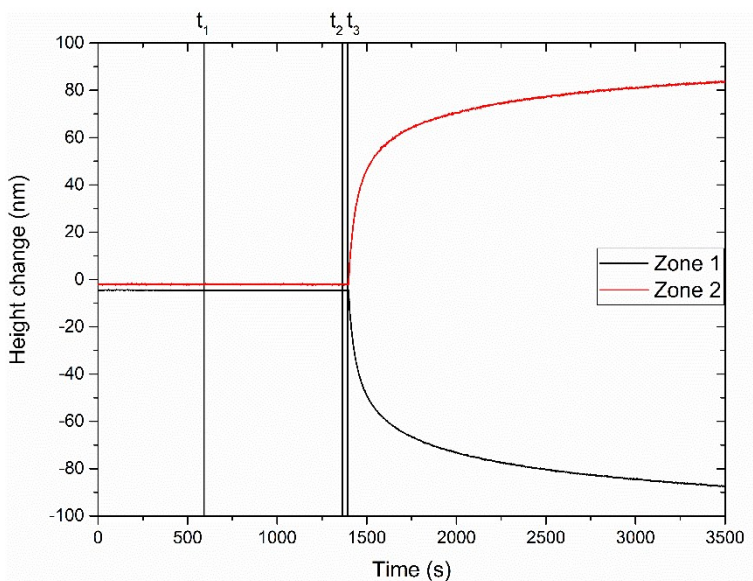


Figure S5: Height change monitored over time with different inputs at  $t_1$ ,  $t_2$  and  $t_3$  indicated with black solid horizontal lines. At  $t_1$  (= 591 s) the rotating stage without polarizer is turned on at  $2.5^\circ \text{ s}^{-1}$ , at  $t_2$  (= 1364 s) the rotating stage is stopped and at  $t_3$  (= 1394 s) the rotating stage without polarizer is turned back on together with the LEDs. The intensity for 365 nm and 455 nm light is  $200 \text{ mWcm}^{-2}$  and  $20 \text{ mWcm}^{-2}$ , respectively.

### Differential scanning calorimetry of the light responsive coating

The temperature at which the experiment is executed has a large influence as visualized in Figure 5. To understand the properties of the coating at the given temperatures, differential scanning calorimetry (DSC) has been performed. In Figure S6, the DSC curve is shown with a temperature range from  $-20^\circ \text{C}$  to  $120^\circ \text{C}$ . A glass transition can be clearly observed at around  $40\text{--}46^\circ \text{C}$ . This is the temperature at which the coating responses most pronounced to rotating linear polarized UV light actuation in presence of blue light.

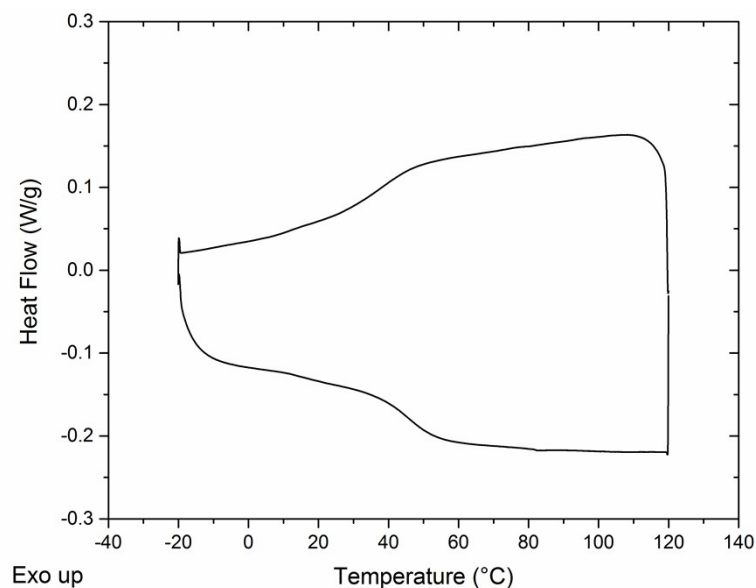


Figure S6: The DSC curve (second heating and cooling trace) of the light responsive coating.

### **Initial topographies of the coating prior to illumination**

For the effect of temperature, the coating was heated to different temperatures and equilibrated at each temperature for a prolonged time. Due to the thermal expansion of liquid crystal networks, the patterned coating will undergo an anisotropic expansion leading to formation of topographies. In Figure S7, the profile of a 20  $\mu\text{m}$  domain coating is shown at different temperatures. Below the glass transition temperature (*i.e.* 46  $^{\circ}\text{C}$ ) the height profile remains relatively unchanged, upon further heating the coating starts to form more pronounced topographies in the same order of sizes as achieved with light exposure.

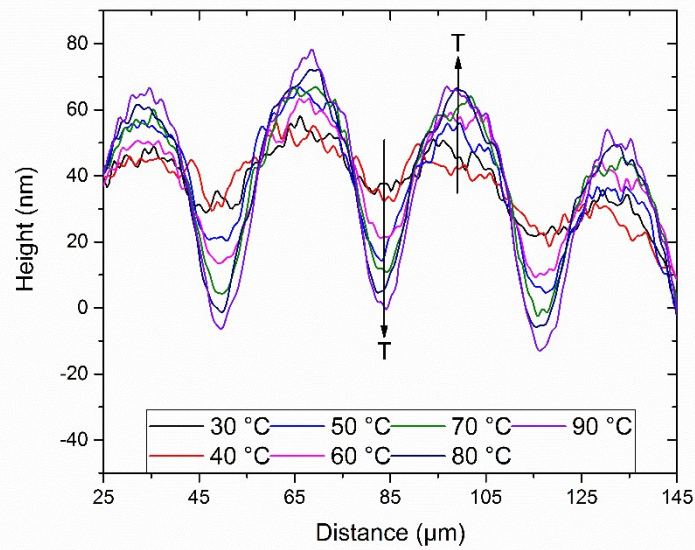


Figure S7: Profile of a 20  $\mu\text{m}$  line patterned coatings at different temperatures.

The profile extraction clearly illustrates the growth of the topographies in function of increasing temperature. For a better illustration of the coatings, Figure S8 shows the 3D illustrations of the coating at different temperatures. As can be seen, most deformations of the coating happen above the glass transition temperature. Changes due to temperature until 50  $^{\circ}\text{C}$  are hardly present. Upon cooling, these height changes are completely reversible.

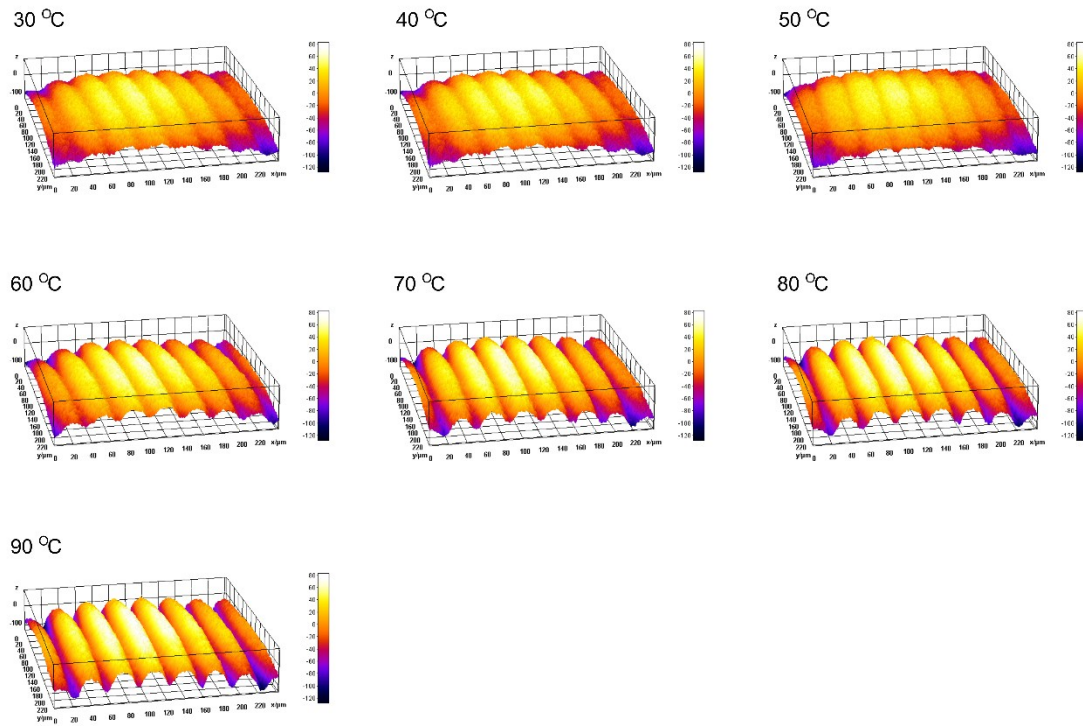


Figure S8: Graphical 3D representations of the initial state of the coating at different temperatures prior to actuation.

### Influence of blue light during relaxation of the topographies

To understand the relaxation of the topographies, a photopatterned coating, with domains oriented planar and orthogonal, is illuminated with unpolarized UV and blue light for a minimum of 10 minutes. Afterwards the unpolarized UV light is turned off. In presence of blue light, the topographies decrease significantly and are returning to their initial quasi-flat state for more than 90% in 30 minutes. In Figure S9 and Figure S10, we show the relative relaxation and the actual height during actuation and relaxation with different irradiance ratios, respectively. In the first case, this ratio is 0, meaning there is no blue light present during and after the actuation with unpolarized UV light.

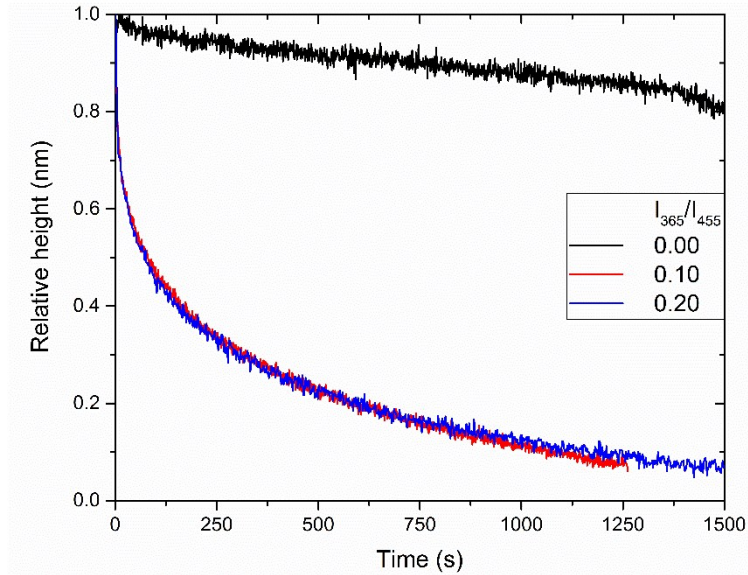


Figure S9: Relative height change during relaxation after an actuation of at least 10 minutes.

From Figure S9, it can be concluded that the presence of blue light is necessary for the relaxation of the topographies. In presence of any amount of blue light compared prior to relaxation, the topographies relax back more than 90 % within 30 minutes. Without the presence of blue light, the topographies will decrease in height slowly over the timespan of days, while an exponential decay is observed in the presence of blue light. In Figure S10, the different normalized height changes are shown prior and during relaxation. Here the time axis is normalized for simplicity. Here the relaxation clearly occurs for any experiment in presence of any blue light. The main difference is the actuation height reached with the different irradiance ratios. An optimal height change is found for a ratio of 0.1.

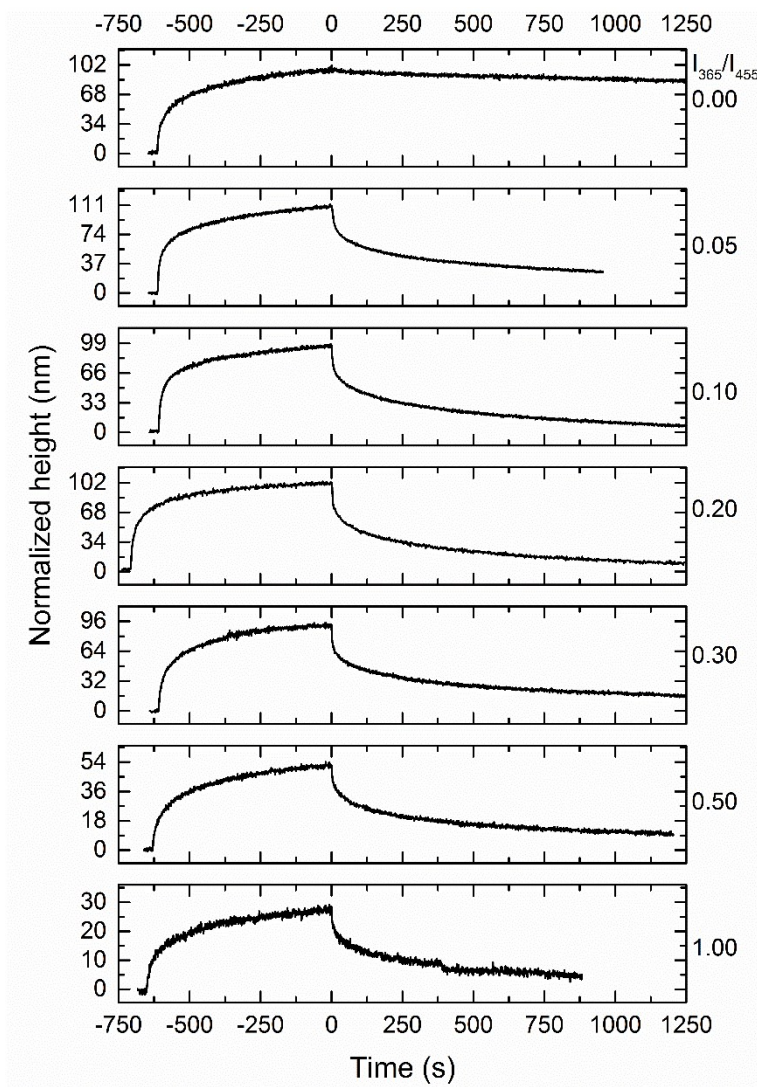


Figure S10: Normalized height changes prior and during relaxation for each of the different irradiance ratios, depicted on the right hand side of the individual graphs.